Electrical conductivity studies of ZnO dispersed PVdF-HFP nanocomposite solid polymer electrolyte for lithium polymer battery applications

O. Padmaraj [a], M. Venkateswarlu [b], N. Satyanarayana [a*]
[a] Department of Physics, Pondicherry University, Pondicherry 605 014, India.
[b] R&D, Amaraja batteries, Thirupathi 517 501, India.

ABSTRACT

Nanocomposite solid polymer electrolyte (NCSPE) films were developed by solution casting method. Polyvinylidene difluoride-co-hexafluoropropylene (PVdF-HFP) as a polymer host, lithium perchlorate ($LiClO_4$) as a salt and ZnO nanoparticles as fillers were used to form the nanocomposite solid polymer electrolyte films. ZnO nanoparticles were synthesized by sol-gel combustion process. XRD, FTIR, DSC and SEM were used to characterize the prepared ZnO nanoparticles and nanocomposite solid polymer electrolyte films. The XRD results showed the formation of amorphous phase with the addition of 17.5 wt% of lithium salt and various wt% of ZnO fillers. The highest conductivity of nanocomposite solid polymer electrolyte at room temperature is found to be 1.043×10^{-3} S/cm for the 17.5 wt% of lithium salt and 3 wt% of ZnO fillers in the polymer film. Also, the lithium ion transference number is estimated for all the NCSPE films and the transference number for the highest conducting composition of NCSPE film is found to be 95%.

Keywords: ZnO nano fillers, sol-gel combustion process, Nanocomposite solid polymer electrolyte, Solution casting method, XRD, FTIR, DSC, SEM, Impedance, Conductivity, Wagner polarization, transference number.

1. INTRODUCTION

Solid polymer electrolytes are used as suitable electrolyte materials in most of the solid state ionic devices, like lithium ion batteries, fuel cells, etc., because of their many advantages over others [1,2]. Many polymers, such as PEO, PAN, PMMA, PVC, PVdF, PVdF-HFP with lithium salts (Li^+X^-) X= ClO_4, PF_6, BF_4, CF_3SO_3 and $(CF_3SO_2)2N^-$ have been developed as solid polymer electrolytes [3, 4]. Among the available polymers, PVdF-HFP has better properties such as high dielectric constant, low crystallinity, lower glass transition temperature, excellent mechanical strength and good electrochemical stability and hence, it has been used as host material for developing good solid polymer electrolyte [5, 6]. In the present work, ZnO nanoparticles were synthesized by sol-gel combustion process for developing the different composition of [(82.5 wt %) PVdF-HFP + (17.5 wt %) $LiClO_4$ + y wt% ZnO, y = 1 to 5% insteps of 1%] nanocomposite solid polymer electrolyte (NCSPE) films by solution casting method.

2. EXPERIMENTAL METHODS

2.1. Synthesis of zinc oxide nanoparticles

Zinc nitrate from s-d fine and citric acid anhydrous from qualigens were used as raw materials for the preparation of ZnO nanocrystalline particles by sol-gel combustion process. By fixing the metal nitrates to citric acid ratio (MN: CA) at 1:1.5, the required amount of zinc nitrate and citric acid were separately dissolved in distilled water. Later, both the solutions were mixed and stirred at 60° C. After half an hour, a little amount of ammonia solution was added drop by drop to the above solution to adjust the pH value at 6 to 7 under continuous stirring at 80 ° C for 6 hours to form the polymeric resin. Finally, the obtained polymeric resin was dried in oven at 50 ° C for 24 hrs and further, it calcined at different temperatures to obtain the ZnO nanoparticles. All the prepared samples were characterized by XRD, FTIR and SEM.

2.2. Preparation of nanocomposite solid polymer electrolyte (NCSPE)

Polyvinylidene difluoride -co- hexafluoropropylene (PVdF-HFP) (Aldrich, Mw=4 x 10^5), $LiClO_4$ (Aldrich) and ZnO nanoparticles were used as the starting materials for the preparation of NCSPE by solution casting method. First, (82.5 wt%) of PVdF-HFP was dissolved in tetrahydrofuron (THF) and stirred continuously for 12 hrs to form a homogeneous solution. Then, separately, 17.5wt% of $LiClO_4$ was dissolved in THF and added to the above polymer solution under continuous stirring for 12 hrs at 60 °C. Also, various amounts of [(y wt%) ZnO, y = 1 to 5% insteps of 1%] ZnO nanoparticles were added to the above mixed solution under continuous stirring. The resultant light viscous solution was poured into a petri dish and the solvent was allowed to evaporate slowly at room temperature for 24 hours. Residual solvents were further removed in a vacuum oven for 24 h at 50 °C.

2.3. Characterization techniques

X-ray diffraction patterns were recorded from 10° to 80° for all the prepared samples using PANalytical X-pertPRO diffractometer (Philips) with Cu-Kα radiation (λ= 0.154060 nm) at 30 mA current and 40 KV voltage. Fourier transform infrared (FTIR) transmittance spectra were recorded for all the prepared samples in the range of 1400 to 400 cm^{-1} using NICOLET 6700 Spectrophotometer with 4 cm^{-1} resolution. DSC curves were recorded for all the prepared samples under the nitrogen atmosphere using differential scanning calorimeter **(DSC Q_{20} instrument)** at 10° C/ min over the temperature range from 30 °C to 250 °C. Scanning electron microscope (SEM) images were captured using Hitachi S4700 for all the prepared samples. The impedance (Z) data were measured at room temperature using

"Novocontrol Impedance frequency analyzer" in the frequency range from 10 MHz to 10 mHz for all the prepared solid polymer electrolyte (SPE) and nanocomposite solid polymer electrolyte (NCSPE) films by sandwiching between the two stainless steel (SS) electrodes as SS/SPE/SS and SS/NCSPE/SS. Lithium ion transference number (t_+) was evaluated at room temperature using Wagner's polarization method for all the prepared SPE and NCSPE films using **'Keithley 617'** programmable electrometer.

3. RESULTS AND DISCUSSION

3.1 ZnO nanoparticles

Figure 1 shows the XRD pattern of the ZnO sample prepared at 700° C along with the standard JCPDS # 036-1451 data. From figure 1, the observed XRD peaks matched with the standard JCPDS # 036-1451 data and confirm the formation of pure crystalline phase of ZnO. The average crystallite size of the ZnO sample was calculated using Scherer formula $t = 0.9\lambda / \beta \cos\theta$ and it is found to be 30 nm. Figure 2 shows the FTIR spectrum of the ZnO nanoparticles. From fig.2, the IR band at 3500 cm^{-1} corresponding to the O–H group. The observed broad band between 548 cm^{-1} and 414 cm^{-1} is attributed to Zn–O vibration mode [7]. Figure 3 shows the SEM image of ZnO powder. From fig.3, it can be seen that the prepared ZnO particles are spherical in shape and the average size of the ZnO particles is found to be ~50 nm. XRD FTIR and SEM results confirmed the formation of pure ZnO nanocrystalline spherical particles prepared by sol-gel combustion method.

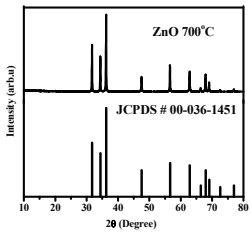

Fig.1

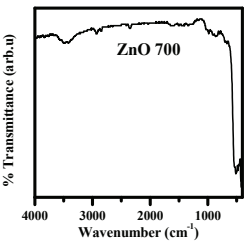

Fig.2

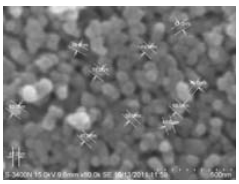

Fig.3

Fig.1. XRD pattern of ZnO sample calcined at 700°C.
Fig.2. FTIR spectra of ZnO sample calcined at 700°C.
Fig.3. SEM image of ZnO powder.

3.2 Nanocomposite solid polymer electrolyte (NCSPE)

Figure 4 shows the XRD patterns of pure PVdF-HFP copolymer, solid polymer electrolyte (82.5 wt% PVdF-HFP + 17.5 wt% $LiClO_4$) and nanocomposite solid polymer electrolyte [(82.5 wt% PVdF-HFP + 17.5 wt% $LiClO_4$ + y wt% ZnO), y = 0 to 5% insteps of 1 wt%] along with the JCPDS data of pure PVdF polymer and XRD pattern of ZnO nanoparticle fillers. From figure 4, the observed XRD pattern of pure PVdF-HFP copolymer showed a low intensity diffraction peaks at 18.5°, 20°, 26.6° and 38.9° over the broad peaks, which correspond to the crystallization phase of pure PVdF and it also conformed by comparing the standard JCPDS # 00-038-1638 data of pure PVdF. The addition of lithium salt [(17.5 wt%) $LiClO_4$] to the (82.5 wt %) PVdF-HFP copolymer host, the XRD peaks are disappeared completely, which indicate the reduction in crystallinity (X_c) and formation of amorphous phase. Further, the intensity of the XRD peaks of the solid polymer electrolyte film decreases drastically with the addition of ZnO filler from 1 wt% to 3 wt% and for further addition of 4 wt% to 5 wt% of ZnO fillers, the XRD peaks starts reappearing. The reduction of diffraction peak intensity may indicate the formation of better amorphous phase through Lewis acid-base interactions between the ZnO nanoparticle and PVdF-HFP copolymer segments. The observed XRD peaks for the addition of ZnO nanofillers of 4 & 5 wt% into solid polymer electrolyte [(82.5 wt %) PVdF-HFP + (17.5 wt %) $LiClO_4$] are compared with the XRD pattern of the prepared ZnO nanoparticle filler and confirmed the formation of crystalline phase of ZnO over the amorphous phase of PVdF-HFP copolymer [8].

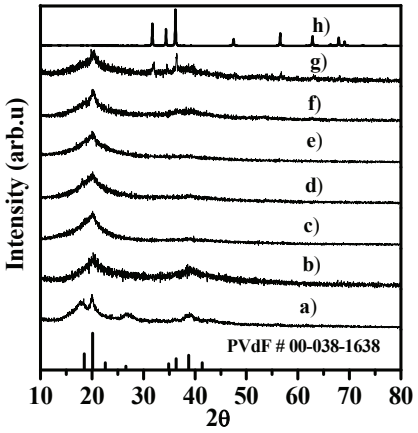

Fig.4. XRD pattern for a) Pure, b) SPE, c) 1wt%, d) 2 wt%, e) 3 wt% f) 4 wt% & g) 5 wt% of NCSPE film.

Figure 5 shows the FTIR spectra of the pure PVdF-HFP, SPE [(82.5 wt% PVdF-HFP + 17.5 wt% $LiClO_4$] and NCSPE [(82.5 wt% PVdF-HFP + 17.5 wt% $LiClO_4$ + 3wt% ZnO] From fig.5, the broad band at 1295 cm^{-1} to 1069 cm^{-1} are assigned to the $–C – F_2$ asymmetric and symmetric stretching mode. The strong vibration bands at 973, 798 and 527 cm^{-1} are assigned to the α-phase of pure PVdF and the bands at 872 and 489 cm^{-1} corresponds to γ and β-phase of PVdF respectively [9]. The absorption band at 761 cm^{-1} is assigned to a rocking vibration, and 612 cm^{-1} to a mixed mode of CF bending and CCC skeletal vibration. The band at 884 cm^{-1} is ascribed to a mixed mode of CH_2 rocking and CF_2 asymmetric stretching vibration. The band at 491 cm^{-1} is attributed to the CF_2 bending mode. Addition of 17.5 wt% LiClO4 into 82.5 wt% PVdF-HFP host, all the characteristic IR bands of PVdF-HFP copolymer frequencies are shifted and also observed the changes in the intensity of IR bands, which may indicate the interaction among the polymer segment with

lithium salt [10]. Further addition of 3 wt% of ZnO in the SPE, the IR bands are shifted and changed, which indicate the formation acid-base interactions between the ZnO nanoparticles and polymer matrix.

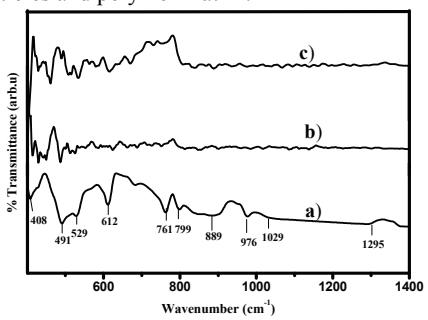

Fig.5. FTIR spectra of a) pure PVdF-HFP polymer, b) SPE with 17.5 wt% $LiClO_4$ and c) NCSPE with 3 wt% ZnO.

Figure 6 shows the DSC curves for pure PVdF-HFP, SPE (82.5 wt% PVdF-HFP + 17.5 wt% $LiClO_4$) and NCSPE (82.5 wt% PVdF-HFP + 17.5 wt% $LiClO_4$ + 3 wt% ZnO). From fig. 6a, the observed two endothermic peaks at 110 ^oC and 146 ^oC are respectively attributed to the removal of absorbed moisture and melting temperature of the PVdF-HFP copolymer. From fig. 6b & 6c, the two endothermic peaks are shifted to the lower temperature compared to fig. 6a, with the addition of (17.5 wt%) $LiClO_4$ salt and 3 wt% ZnO filler in the PVdF-HFP / LiClO4 / ZnO system respectively. This may enhance the flexibility of polymer chains and hence, decreased the crystallinity of polymer host. From the figure 6, it is observed that the enthalpy (ΔH_m) of melting point of the nanocomposite solid polymer electrolyte found to be a minimum value of 7.75 J/g with 3 wt % of ZnO nanofiller, compared to 10.37 J/g for solid polymer electrolyte with 17.5 wt% of lithium salt and 15.35 J/g for the pure PVdF-HFP copolymer host. The observed enthalpy values, the percentage of crystallinity (X_c) were calculated for pure polymer, solid polymer electrolyte and nanocomposite solid polymer electrolyte using $X_c\ \% = \Delta H_s / \Delta H^* \times 100$ where, $\Delta H^* = 104.7$ J/K, the melting enthalpy of the crystalline PVdF-HFP polymer and their respective values are 14.66%, 9.90% and 7.40%. The gradual decrease in enthalpy (ΔH_m) and crystallinity (X_c%) values with the addition of lithium salt and filler indicate an enhancement in the amorphous phase of polymer host, which may help to enhance the ionic conductivity of nanocomposite solid polymer electrolyte (NCSPE) [11].

Figure 7 shows the SEM images of the prepared pure PVdF-HFP polymer, solid polymer electrolyte (82.5 wt% PVdF-HFP + 17.5 wt% $LiClO_4$) and nanocomposite solid polymer electrolyte with 3 wt % of ZnO ceramic fillers. In fig.7a, the image of pure PVdF-HFP film showed rough and highly compact structure without pores nature, which may be due to the presence of crystalline phase in the PVdF-HFP polymer matrix. With the addition of lithium salt (17.5 wt %) into the pure PVdF-HFP polymer host, the surface of the polymer film showed highly smooth and porous structure compared with the pure polymer as shown in fig. 7b [5]. The smooth and pores nature might be due to the reduction of crystallinity in the PVdF-HFP polymer matrix and also to increase the segmental motion of polymer chain by the addition of lithium salt as well as solvent evaporation [6]. The addition of 3 wt% of ZnO fillers into (82.5) wt% PVdF + (17.5) wt% $LiClO_4$ electrolyte film, resulted in improved the pores and smooth morphology due to the interactions between ZnO nanoparticles, PVdF-HFP and $LiClO_4$ as shown in fig. 7c.

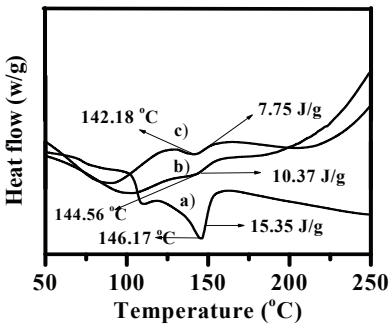

Fig.6. DSC curves for a) pure, b) SPE & c) NCSPE

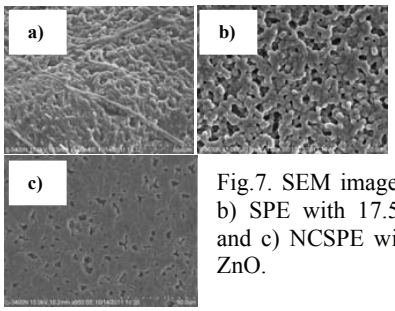

Fig.7. SEM images of a) pure, b) SPE with 17.5 wt% of Li and c) NCSPE with 3 wt% of ZnO.

Figure 8 shows the complex impedance spectra of pure and various wt% (1 to 5wt% insteps of 1) of ZnO dispersed solid polymer electrolyte [(82.5 wt% PVdF-HFP + 17.5wt% $LiClO_4$) films. From the impedance spectra, the intercept on the real axis gives the electrolyte resistance. The conductivity for each composition of SPE & NCSPE was calculated using the following equation $\sigma = (t/A)\ (1/R_b)$ S/cm, where t is the thickness of the electrolyte sample, A is the area of cross section of electrodes and R_b is the electrolyte resistance.

Figure 9 shows the conductivity (σ) Vs ZnO content of the nanocomposite solid polymer electrolyte films. From fig.9, the conductivity increases with the addition of nanofiller upto 3 wt% of ZnO and further addition of 4 & 5 wt% of ZnO, the conductivity (σ) decreases at room temperature. The highest conductivity is found to be 1.043×10^{-3} Scm^{-1} for the NCSPE with 3 wt % ZnO nanofiller. The enhancement in the conductivity may be due to the addition of ZnO nano fillers, which may be acting as a solid plasticizer and also an electrolyte dissociation promoter. These interactions lead to give the structural modifications and also promote the salt dissociation and thus, may help to enhance the conductivity. Further, addition of 4 and 5 wt % of ZnO ceramic fillers in

the optimized SPE, the conductivity was decreased. The decrease in conductivity may be consider as the blocking effect of ion transport in the conduction pathways, which may be due to the aggregation of ZnO nanoparticles, suggesting that the number of available charge carriers for the ionic conduction is decreased. These results are also confirmed with the observed XRD peaks for the 4 & 5 wt% of the ZnO filler in NCSPE. Hence, conductivity result indicate that the developed nanocomposite solid polymer electrolyte with 3 wt% of ZnO nanofiller could be a good promising electrolyte material for lithium polymer batteries as well as any other ionic device applications. Further, its ionic nature is confirmed by measuring the ionic transference number [12].

3.3 Lithium ion transference number

Figure 10 shows the measured current Vs time plot for the highest conducting NCSPE (82.5 wt% PVdF-HFP + 17.5 wt% $LiClO_4$ + 3 wt% ZnO) film. In the plot, initially, current shows maximum (called total current I_T) and starts decreasing with time, finally, it reaches to saturation. The extrapolation of the saturation curve to the Y-axis gave the electronic current (I_{elec}). The transference numbers due to ion (t_{ion}) and due to electron (t_{ele}) were calculated using the equations $t_{elec} = I_e/I_T$ & $t_{ion} = 1-t_{elec}$. The value of ionic transference numbers (t_{ion}) for the nanocomposite solid polymer electrolyte [(82.5 wt%) PVdF-HFP + (17.5 wt%) $LiClO_4$ + (3 wt%) ZnO] film is found to be 0.95. This implies that the charge transport in these nanocomposite solid polymer electrolyte films is predominantly due to ions, and a negligible contribution comes from the electrons. Hence, the prepared highest conducting NCSPE can be good ion conducting electrolyte film and it can be potential electrolyte for all solid state lithium ion batteries as well as other ionic devices [13].

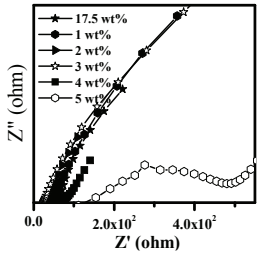

Fig.8

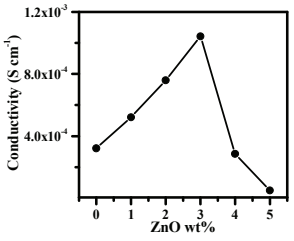

Fig.9

Fig.8.Complex impedance spectra of SPE & NCSPE with different wt% of ZnO.
Fig.9. Conductivity Vs ZnO content plot of NCSPE.
Fi.10. Current Vs time plot for 3 wt% of NCSPE.

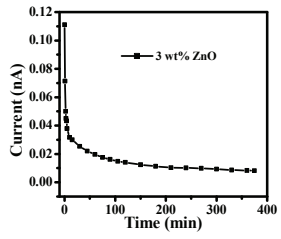

Fig.10

4. CONCLUSION

Pure and various wt% (1 to 5wt% insteps of 1) of ZnO dispersed solid polymer electrolyte [(82.5 wt% PVdF-HFP + 17.5wt% $LiClO_4$) films were developed using solution casting method. The reduction in the crystallinity of PVdF-HFP with the addition of $LiClO_4$ & ZnO is confirmed from the analysis of the measured XRD, FTIR, DSC, SEM results, which resulted in significant enhancement of the ionic conductivity in the nanocomposite solid polymer electrolyte. The observed high ionic conductivity 1.043 x 10^{-3} S/cm at room temperature in NCSPE is evaluated from the measured impedance and transference number data. Hence, the newly developed highest ion conducting nanocomposite solid polymer electrolyte [82.5 wt% PVdF-HFP + 17.5 wt% $LiClO_4$ + 3 wt% ZnO] can be potential electrolyte for lithium batteries as well as other ionic device applications.

Acknowledgements: Dr. N. Satyanarayana gratefully acknowledges AICTE, CSIR, DST, UGC and DRDO, government of India for financial support through major research project grants.

***Correspondence Author Tel:** 0413-2654 404.

E-mail: nallanis2011@gmail.com,

REFERENCE

[1] Yan-Jie Wang, Dukjoon Kim, Electrochimica Acta 52 (2007) 3181.
[2] A. Manuel Stephen, K.S. Nahm, Polymer 47 (2006) 5952.
[3] Jingyu Xi, Xinping Qiu, Sixum Zheng, Xiaozhen Tang, Polymer 46 (2005) 5702.
[4] A. L. Sharma, Awalendra K. Thakur, Journal of Applied Polymer Science 118 (2010) 2743.
[5] V. Aravindan, P. Vickraman, European Polymer Journal 43 (2007) 5121.
[6] Chun-Guey Wu, Ming-I.Lu, Chung-Chih Tsai, Journal of Power source 159 (2006) 295-300.
[7] Yuan Cao, Bolin Liu, Rui Huang, Zhining Xia, Song Ge, Materials Letters 65 (2011) 160–163.
[8] Huan-Ming Xiong, Xu Zhao, and Jie-Sheng Chen, Journal Phys. Chem. B 105 (2001) 10169-10174.
[9] M. Deka, A. Kumar, Journal of Power Sources 196 (2011) 1358.
[10] Deng Zhang, Ruoshi Li, Tao Huang, Aishui Yu, Journal of power sources 195 (2010) 1202-1206.
[11] Lishi Wang, Wensheng Yang, Jian Wang, David G. Evans, Solid state Ionics 180 (2009) 392-397.
[12] Jae-Deok Jeon, Seung-Yeop Kwak, and Byung-Won Cho, Journal of the Electrochemical Society, 152 (8) (2005) A1583-A1589.
[13] Balaji Bhargav, V. Madhu Mohan, A. K. Sharma, V. V. R. N. Rao, Ionics 13 (2007) 173–178.